PCCP

PAPER

View Article Online
View Journal | View Issue

Cite this: *Phys. Chem. Chem. Phys.*, 2018, **20**, 9847

When is electronic friction reliable for dynamics at a molecule–metal interface?

Alec J. Coffman * and Joseph E. Subotnik

Received 8th December 2017,
Accepted 16th March 2018

DOI: 10.1039/c7cp08249e

rsc.li/pccp

We investigate rates of electron transfer for generalized Anderson–Holstein models in the limit of weak molecule–metal coupling, using both surface hopping and electronic friction dynamics in one and two dimensions. Overall, provided there is an external source of friction, electronic friction can sometimes perform well even in the limit of small metal–molecule coupling and capture nonadiabatic effects. However, we show that electronic friction dynamics is likely to fail if there is a competition between nonequivalent pathways. Our conclusions provide further insight into the recent observation by Ouyang *et al.*, [*J. Chem. Theory Comput.*, 2016, **12**, 4178] regarding the applicability of Kramer's theory in the adiabatic limit to recover Marcus theory in the nonadiabatic limit.

I. Introduction

Many critical electron transfer (ET) phenomena occur in the nonadiabatic limit, where the Born–Oppenheimer approximation is no longer valid. One such case is that of a molecule near a metal surface,[1–5] where an electron can transfer between a molecule and metal at relatively long distances. Such an ET process is at the heart of many electrochemical systems,[6–9] molecular junctions, and even some scattering problems.[10,11] In general, these nonadiabatic dynamics are challenging to model quantitatively because the systems are very large.

In this work, we focus exclusively on the high temperature limit, $\hbar\omega < kT$ (ω being a typical nuclear frequency), so as to allow for a separation of nuclear and electronic motion and a classical treatment of the nuclear degrees of freedom (DoFs). There are today two common approaches for modeling such coupled nuclear-electronic dynamics: surface hopping (SH) and generalized electronic friction with Langevin dynamics (EF-LD). First, according to SH, one propagates dynamics independently on two diabatic surfaces, while the influence of the metal surface acts as a coupling between impurity occupied/unoccupied diabatic states.[12] Second, the EF-LD method entails running effectively adiabatic dynamics along a potential of mean force (PMF), subject to an external friction and random force (that arises from the continuum of electronic states in the bath[13]). Many electronic friction models have been implemented, based on bootstrapping,[14] perturbation theory in quasi-classical or reduced coordinates,[15–18] bosonization techniques,[19,20] a nonequilibrium Green function approach,[21–25] and influence functionals and more generally path integrals.[26–28] Recently, our group has demonstrated that all of these results emerge from one universal electronic friction tensor[29–31] based on the quantum-classical Liouville equation[32,33] plus projection operators.[34,35] In general, because the SH method is a perturbative treatment in Γ, the hybridization function that describes the elctron-metal coupling, SH should be valid only in the limit where the electron-metal coupling is small compared to kT ($\Gamma < kT$). By contrast, EF-LD is based on a slow velocity approximation and should require fast equilibration, meaning that $\Gamma > \hbar\omega$ (and small electron–phonon couplings). Recent work has shown that there are ways to bridge the gaps between the two methods, *i.e.* by employing SH trajectories moving along broadened diabatic surfaces,[36] or by discretizing the continuum of electronic states and assuming independent single electron states using an independent-electron surface hopping (IESH) method.[37,38] For increased accuracy, one can incorporate nuclear quantum effects into a master equation.[39,40] For efficient dynamics, a local density approximation can be used; see the recent studies by Juaristi and Reuter where electronic friction was used to study the relaxation of CO on Cu and N on Ag.[41]

Now, despite the formal arguments above, in a previous work Ouyang *et al.*[42] found a very curious result: EF-LD dynamics unexpectedly agree with SH dynamics in the limit $\Gamma < \hbar\omega$, as long as there is (1) a sufficiently large exit barrier from one diabatic well with a single exit channel, (2) a source of external (nuclear/phononic) friction, and (3) the coupling Γ doesn't depend on position. Under these restrictive conditions, which preclude any important excited state dynamics, Marcus theory is approximately equal to Kramer's theory in the small Γ limit.[42] Our goal in the present article is to further examine the EF-LD approach and assess its performance in this small Γ limit. It is clear that electronic friction cannot agree with surface hopping in the absence of external friction for weak-molecule metal coupling,[12]

Department of Chemistry, University of Pennsylvania, Philadelphia, Pennsylvania 19104, USA. E-mail: alecja@sas.upenn.edu

as shown recently for a 2-D scattering model,[43] and yet what if we relax the other two conditions? How will EF-LD perform? We will be particularly interested in multidimensional problems where multiple channels are possible, as well as violations of the Condon approximation.

To make progress, our approach will be to construct several generalized Anderson–Holstein model[44,45] problems, with non-Condon effects. The AH model is the simplest model possible for studying an electronic impurity coupled to a bath of phonons and electrons, and is often used to quantify ET near a metal surface. Our generalized AH model will employ two diabatic potential energy surfaces (PESs), where the two PESs correspond to the impurity being either occupied or unoccupied, and will be of the form

$$H = H_s + H_b + H_c \tag{1a}$$

$$H_s = E(\mathbf{x})d^\dagger d + V_0(\mathbf{x}) + \sum_{\alpha=1}^{N}\frac{p_\alpha^2}{2m_\alpha} \tag{1b}$$

$$H_b = \sum_k (\varepsilon_k - \mu)c_k^\dagger c_k \tag{1c}$$

$$H_c = \sum_k W_k(\mathbf{x})\left(c_k^\dagger d + d^\dagger c_k\right) \tag{1d}$$

$$\Gamma(\varepsilon, \mathbf{x}) = 2\pi\sum_k |W_k(\mathbf{x})|^2\delta(\varepsilon_k - \varepsilon). \tag{1e}$$

Here, μ is the chemical potential, W_k is the coupling between the bath and system modes, Γ is the hybridization function, V_0 is the impurity unoccupied diabatic state, E is the difference in energy between unoccupied and occupied states, and $c_k(c_k^\dagger)$, $d(d^\dagger)$ are the annihilation (creation) operators in the bath and system, respectively. We utilize a small molecule–metal coupling ($\Gamma < kT$) where SH must be reliable regardless of non-Condon contributions. In this regime we will be able to benchmark EF-LD dynamics against SH dynamics. In what follows, we will construct three model Hamiltonians with different forms for E, V_0, and Γ. These three Hamiltonians will be designed to tease out how non-Condon effects can influence the final dynamics.

The organization of this paper is as follows. In Section II we present the models under investigation and we define the requisite theory and formulae needed to carry out the dynamics being studied. We will then present the results in Section III, discuss our results in Section IV, and conclude in Section V.

II. Theory

We begin by introducing three different generalized AH model problems for analyzing dynamics. Thereafter, we will briefly review how to propagate SH and EF-LD trajectories.

A. Models

1. Model A, two minima in one dimension. Our first model is inspired by conical intersections in solutions, where the diabatic coupling is zero at the actual crossing point. Thus, we define two diabatic PESs,

$$V_0(x) = \frac{1}{2}m\omega^2 x^2 \tag{2a}$$

$$V_1(x) = \frac{1}{2}m\omega^2(x-g)^2 + \Delta G^\circ. \tag{2b}$$

$V_0(x)$ and $V_1(x)$ are the potentials corresponding to an impurity unoccupied or occupied and ΔG° is the free energy difference between the two states; x is the reaction coordinate. These PESs are plotted in Fig. 1(a). The difference in energy as a function of position is

$$E(x) = V_1(x) - V_0(x) = \frac{1}{2}m\omega^2\left(g^2 - 2xg\right) + \Delta G^\circ. \tag{3}$$

We work in the wide band approximation, and the density of states weighted metal–molecule coupling between these two diabats is chosen to be

$$\Gamma(x) = \Gamma_1\left(\Gamma_0 + \frac{K(x-d)^2}{1+K(x-d)^2}\right) \tag{4}$$

where $d = \frac{g}{2} + \frac{\Delta G^\circ}{m\omega^2 g}$ is the x value that minimizes $E(x)$, the crossing point of the two diabatic PESs. Note that $\Gamma(x)$ is minimized at $x = d$, see Fig. 1(b).

2. Model B, two minima in two dimensions. For our second model problem, we introduce another spatial dimension (y) and

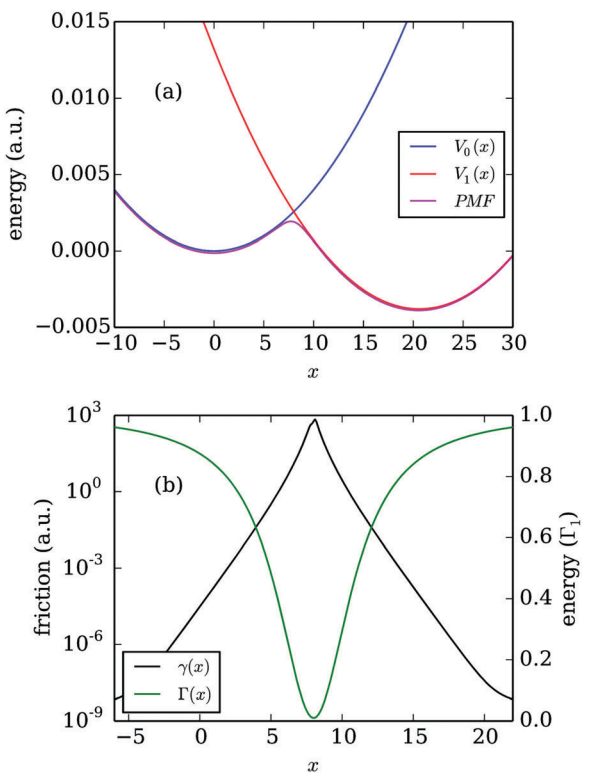

Fig. 1 (a) Diabatic potentials (eqn (2)) and PMF (eqn (16)) for model A. The crossing point is located at $x = 8$. (b) $\Gamma(x)$ and $\gamma(x)$ as a function of position ($\Gamma(x)$ is in units of Γ_1), $\Gamma_0 = 0.01$, $K = 0.1$.

modify the molecule–metal coupling so as to investigate how the dynamics change when Γ depends on y (rather than the reaction coordinate x). To visualize these potentials and couplings, see Fig. 3(a) and (b). The two diabats for this model are

$$V_0(x,y) = \frac{1}{2}m\omega^2(x^2+y^2) \tag{5a}$$

$$V_1(x,y) = \frac{1}{2}m\omega^2\left((x-g)^2+y^2\right) + \Delta G^\circ. \tag{5b}$$

The coupling is now chosen to be

$$\Gamma(y) = \Gamma_0 + \Gamma_1 e^{-\alpha(y-\delta)^2} \tag{6}$$

which results in a coupling that is approximately Γ_0 far from δ and $\Gamma_1 + \Gamma_0 \approx \Gamma_1 (\Gamma_1 \gg \Gamma_0)$ at $y = \delta$.

3 Model C, three minima in two dimensions. Our final model problem considers a case with three minima located near the following points: the reactant minima is centered near $\mathbf{r}_1 = (0, 0)$ and the product minima are near $\mathbf{r}_2 = (g, y_A)$ or $\mathbf{r}_3 = (g, -y_A)$. With three minima, one can now analyze the relative probabilities of $\mathbf{r}_1 \rightarrow \mathbf{r}_2$ and $\mathbf{r}_1 \rightarrow \mathbf{r}_3$. The reactant (unoccupied) diabat is chosen to be the same as V_0 from eqn (5a), while the product (occupied) diabat V_1 is as follows:

$$V_1(x,y) = \frac{1}{2}m\left(\omega^2(x-g)^2 + \omega_y{}^2\left(y^2 + y_A{}^2\right)\right) + \frac{\Delta G_L^\circ + \Delta G_R^\circ}{2} - \sqrt{\left(m\omega_y{}^2 y y_A + \frac{\Delta G_L^\circ - \Delta G_R^\circ}{2}\right)^2 + \varepsilon^2}. \tag{7}$$

Obviously, the product holds two minima that are centered at the same position in the x-direction (at $x = g$) but with two possibilities in the y direction (roughly $y = \pm y_a$). ε is a small parameter chosen as 10^{-6} to ensure that the diabatic potential is smooth. ΔG_L° is roughly the energy difference between the minima of V_0 and the minima located at $-y_A$, while ΔG_R° is roughly the energy difference between the minima of V_0 and the minima located at y_A. The coupling in this model is expressed as a logistic function,

$$\Gamma(y) = \Gamma_0 + \frac{\Gamma_1 - \Gamma_0}{1 + e^{-\kappa(y-\eta)}} \tag{8}$$

where $\Gamma_1 \gg \Gamma_0$ and we chose $\eta = 1$ which ensures the coupling is $\approx \Gamma_1$ near the minima centered at $+y_A$, whereas the coupling is $\approx \Gamma_0$ at the minima centered at $-y_A$. To visualize these potentials and couplings, see Fig. 4(a and b). This model provides a mechanism to study dynamics in the case where the reaction and coupling coordinates are mixed, as well as when multiple exit channels are present.

B. Dynamics

We now review the relevant dynamics protocols.

1. Surface hopping. There are two necessary prerequisites when performing SH dynamics, the small coupling limit ($\Gamma < \hbar\omega$) and the high temperature limit ($\hbar\omega < kT$). The basic premise of SH is that one runs dynamics along individual diabatic surfaces with hops between surfaces. We define the phase space probability densities for the nuclear DoFs as $P_0(\mathbf{x},\mathbf{p},t)$ and $P_1(\mathbf{x},\mathbf{p},t)$ at time t, where $P_0(P_1)$ is the probability density for the electronic impurity to be unoccupied (occupied), assuming the nuclei are at position $\mathbf{x}$ with momentum $\mathbf{p}$. The time evolution of these probability densities is given by the following equations

$$\frac{\partial P_0(\mathbf{x},\mathbf{p},t)}{\partial t} = \nabla_x V_0(\mathbf{x},\mathbf{p})\cdot\nabla_p P_0(\mathbf{x},\mathbf{p},t) - \frac{p}{m}\nabla_x P_0(\mathbf{x},\mathbf{p},t) + \gamma_{0\rightarrow 1}P_0(\mathbf{x},\mathbf{p},t) - \gamma_{1\rightarrow 0}P_1(\mathbf{x},\mathbf{p},t) \tag{9a}$$

$$\frac{\partial P_1(\mathbf{x},\mathbf{p},t)}{\partial t} = \nabla_x V_1(\mathbf{x},\mathbf{p})\cdot\nabla_p P_1(\mathbf{x},\mathbf{p},t) - \frac{p}{m}\nabla_x P_1(\mathbf{x},\mathbf{p},t) + \gamma_{0\rightarrow 1}P_0(\mathbf{x},\mathbf{p},t) - \gamma_{1\rightarrow 0}P_1(\mathbf{x},\mathbf{p},t) \tag{9b}$$

where $\gamma_{0\rightarrow 1}(\gamma_{1\rightarrow 0})$ is the hopping rate from surface 0 to 1 (1 to 0)

$$\gamma_{0\rightarrow 1} = \frac{\Gamma(\mathbf{x})}{\hbar} f(E(\mathbf{x})) \tag{10a}$$

$$\gamma_{1\rightarrow 0} = \frac{\Gamma(\mathbf{x})}{\hbar}(1 - f(E(\mathbf{x}))) \tag{10b}$$

and $f(E(\mathbf{x}))$ is the fermi function, $f(E(\mathbf{x})) = \frac{1}{1+e^{\beta(E(\mathbf{x}))}}$, $\beta = (k_B T)^{-1}$. These SH dynamics are very different from Tully's energy conserving fewest switches surface hopping method; in the present case, the system is open with respect to energy flow between the system and bath and therefore energy conservation is not imposed with each hop.

2. Electronic friction. We first define some mathematical identities that are needed for the presentation of EF-LD. For a general problem on a metal surface with multiple nuclear degrees of freedom, the relevant EF-LD dynamics take the form:[46]

$$-m_\alpha \ddot{x}_\alpha = -F_\alpha + \sum_\beta \gamma_{\alpha\beta}\dot{x}_\beta + \delta f_\alpha(t). \tag{11}$$

Here α is an index for a nuclear DoF and F_α is the mean force

$$F_\alpha = -\left(\frac{\partial V_0}{\partial x_\alpha} + \int_{-\Lambda}^{\Lambda}\frac{d\varepsilon}{2\pi}\left(\frac{\partial E}{\partial x_\alpha} + \frac{(\varepsilon - E)}{\Gamma}\frac{\partial \Gamma}{\partial x_\alpha}\right)A(\varepsilon,\mathbf{x})f(\varepsilon)\right). \tag{12}$$

$\gamma_{\alpha\beta}$ is the $\alpha\beta$ element of the electronic friction tensor

$$\gamma_{\alpha\beta} = \frac{\hbar}{2}\int\frac{d\varepsilon}{2\pi}\left(\frac{\partial E}{\partial x_\alpha} + \frac{(\varepsilon - E)}{\Gamma}\frac{\partial \Gamma}{\partial x_\alpha}\right) \times \left(\frac{\partial E}{\partial x_\beta} + \frac{(\varepsilon - E)}{\Gamma}\frac{\partial \Gamma}{\partial x_\beta}\right) \times A(\varepsilon,\mathbf{x})^2\frac{f(\varepsilon)(1-f(\varepsilon))}{kT} \tag{13}$$

and $\delta f_\alpha(t)$ is the random force with associated correlation function $D_{\alpha\beta}\delta(t-t') = \langle \delta f_\alpha(t)\delta f_\beta(t')\rangle$,

$$D_{\alpha\beta} = \hbar\int\frac{d\varepsilon}{2\pi}\left(\frac{\partial E}{\partial x_\alpha}+\frac{(\varepsilon-E)}{\Gamma}\frac{\partial\Gamma}{\partial x_\alpha}\right) \times\left(\frac{\partial E}{\partial x_\beta}+\frac{(\varepsilon-E)}{\Gamma}\frac{\partial\Gamma}{\partial x_\beta}\right) \times A(\varepsilon,\mathbf{x})^2 f(\varepsilon)(1-f(\varepsilon)). \quad (14)$$

In the above equations $A(\varepsilon,\mathbf{x})$ is the spectral function,

$$A(\varepsilon,\mathbf{x}) = \frac{\Gamma(\mathbf{x})}{(\varepsilon-E(\mathbf{x}))^2+\left(\frac{\Gamma(\mathbf{x})}{2}\right)^2} \quad (15)$$

and Λ is the electronic bandwidth, which is chosen such that $\Lambda \gg \Gamma$. When the Condon approximation holds $\left(\frac{\partial\Gamma}{\partial x_\alpha}=0\right)$ the above equations simplify considerably. The PMF is given by

$$V_{\mathrm{PMF}}(\mathbf{x}) = -\int_{\mathbf{x}_0}^{\mathbf{x}} F(\mathbf{x}')\cdot d\mathbf{x}' \quad (16)$$

where F is given in eqn (12). For graphical purposes, V_{PMF} can be evaluated numerically on a grid.

C. Simulation details

Below, we wish to study dynamics in the presence of a thermal environment. Thus, we will include an additional non-electronic source of friction, γ_n. Trajectories for each model are initialized on diabat V_0 with a Boltzmann distribution of position and velocity. Rates for SH were obtained by fitting the impurity population as a function of time with an exponential, while rates for EF-LD were found by fitting the position as a function of time to an exponential. Unless stated otherwise, 200 trajectories were run for both SH and EF-LD simulations, and all simulations were performed with $\Gamma_1 = 0.0001$, $m = 2000$, $\omega = 0.0002$, $g = 20.6097$, $\Delta G^\circ = -0.0038$, $\gamma_n = 2m\omega = 0.4$, $\Lambda = 0.1$, and $kT = 0.00095$. All parameters are in atomic units.

III. Results

A. Model A

In Fig. 1(b) we plot $\Gamma(x)$ and $\gamma_e(x)$ for model A. Note that the friction increases dramatically near the crossing point, $x = d$, which should significantly reduce the rate of barrier crossings according to EF-LD. Fig. 2(a) shows the ratio of rates obtained from SH *versus* EF-LD, $\frac{k_{\mathrm{SH}}}{k_{\mathrm{EF}}}$, for a wide set of parameters for model A. Under a broad set of $\Gamma(x)$ parameterizations, EF-LD underestimates the rate by as much as an order of magnitude compared to SH. One might suppose that the rates from SH are higher due to the ability for hops to occur at positions far from the crossing point, where $\Gamma(x)$ is at a minimum, whereas all EF-LD trajectories must pass through the crossing point region where the friction is very large. To test this, we looked at the positions where hops from diabat 0 to diabat 1 were most likely to occur. Fig. 2(b) shows a histogram of such positions, for the case $\Gamma_0 = 0.01$, $K = 0.1$ where the EF-LD and SH rates are very different. Note that, as expected, the hops occur far from the crossing point, $x = d$, and form a bimodal distribution. Indeed, by investigation one concludes that EF-LD and SH disagree more as the hopping distribution becomes more bimodal.[47]

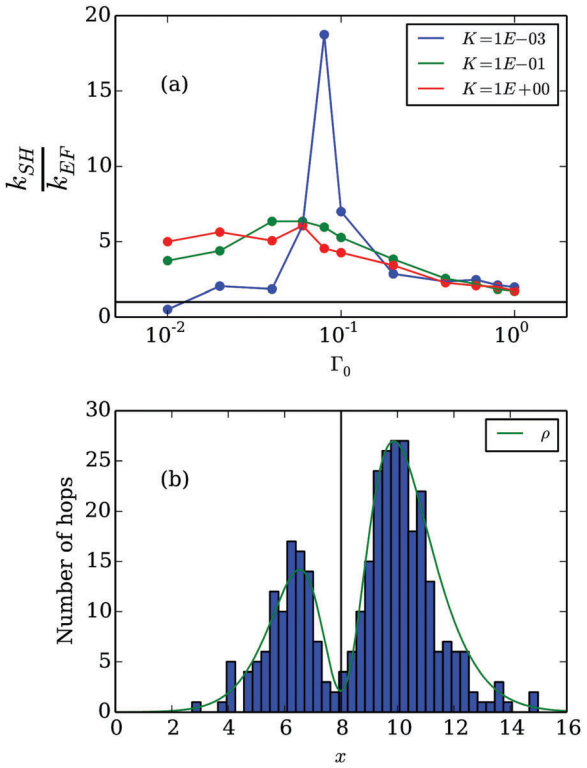

Fig. 2 Results from model A. (a) Ratio of rates of ET from SH and EF-LD for multiple combinations of parameters K and Γ_0. SH and EF-LD rates agree in the limit of large Γ_0, since the positional dependence weakens as Γ_0 increases. (b) Histogram of positions where hops occur for the parameters in Fig. 1(b). The green trace, ρ, is a rescaled distribution capturing the probability of being at a given position multiplied by the hopping probability from diabat 0 to diabat 1: $\rho(x) = Ne^{-\beta V_0(x)} \times \Gamma(x) \times f(E(x))$. In general, EF-LD appears to disagree with SH when the hopping probability is bimodal.

B. Model B

Having analyzed how reactions proceed when the Condon approximation is violated along a reaction coordinate, we now address how reactions proceed when the Condon approximation is violated in an orthogonal coordinate (*i.e.* the reaction coordinate is x but Γ depends on y). The PMF for model B is shown in Fig. 3(a). While the PMF is not drastically affected by the y dependence of $\Gamma(y)$, the main dynamical effects can be seen in the friction. Fig. 3(b) shows the "effective" force on a particle in the negative x-direction, assuming the velocity in both coordinates is equal to the root-mean square velocity, chosen so as to illustrate the force under a typical velocity. Unlike the one-dimensional case, EF-LD allows for barrier crossing in the direction of the reaction coordinate through a narrow channel where Γ is maximized and the friction is minimized.

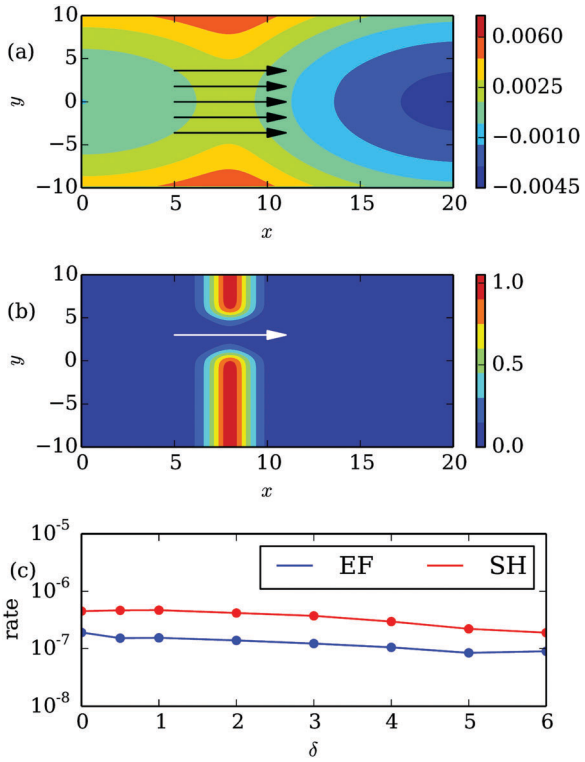

Fig. 3 (a) PMF for model B. Parameter values are $\Gamma_0 = 1e-5$, $\alpha = 0.5$, $\delta = 3$. The black arrows indicate the overall reaction coordinate. (b) Normalized effective force on a particle in the negative x-direction for the parameterization in (a), assuming a velocity $v_x = v_y = v_{rms} = \sqrt{\frac{3kT}{m}}$. See eqn (11)–(13); here we plot $\frac{\partial V_0}{\partial x} - F_x + \gamma_{xx}v_x + \gamma_{xy}v_y$. While the PMF predicts equally likely crossings over a wide set of y values, the frictional effects shown in (b) suggest that there is only a narrow channel through which trajectories can pass from the left minima to the right minima. (c) Rates for SH and EF-LD for the same model as (a), as a function of δ. Note the success of the EF-LD approach in effectively recovering the correct SH rate.

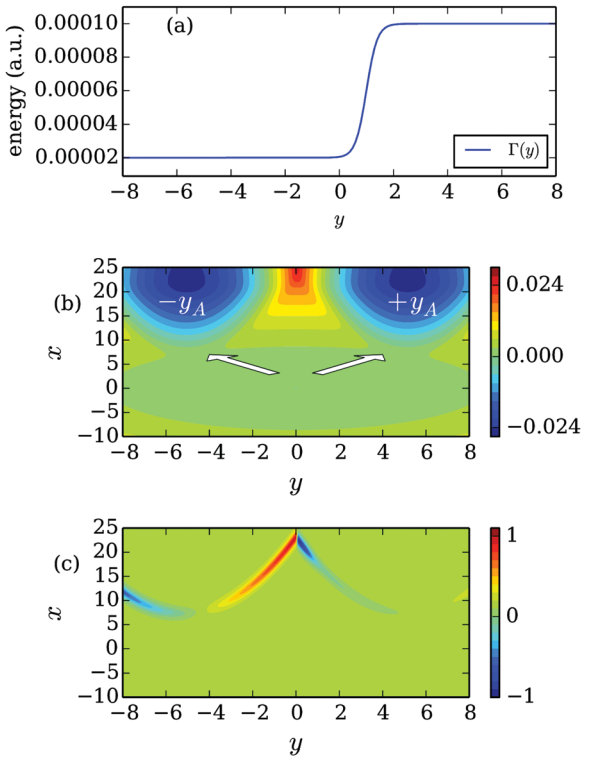

Fig. 4 (a) $\Gamma(y)$ for model C; the metal–molecule coupling is stronger for the right minima *versus* the left minima. (b) PMF for model C, $\omega_y = 5\omega = 0.001$, $\Delta G^\circ_R = \Delta G^\circ_L = -0.0038$, $y_A = 5$, $\Gamma_0 = 2e-5$, $\kappa = 5$, $\eta = 0$. The arrows show the two possible reactive pathways to the product minima at $-y_A$ or $+y_A$. For $\Delta G^\circ_L = \Delta G^\circ_R$, because of $\Gamma(y)$, we expect more trajectories to propagate towards the $+y_A$ well rather than the $-y_A$ well. (c) Normalized effective force on a particle in the negative x-direction for the parameterization in (a), assuming a velocity $-v_y = v_x = v_{rms} = \sqrt{\frac{3kT}{m}}$. See eqn (11)–(13): here we plot $\frac{\partial V_0}{\partial x} - F_x + \gamma_{xx}v_x + \gamma_{xy}v_y$. Note the frictional barrier between the two minima in (c), as well as a frictional preference for trajectories to move towards the $+y_A$ well rather than the $-y_A$ well.

In Fig. 3(c) we plot the rates for SH and EF-LD as a function of δ. Although EF-LD slightly underestimates the rate compared to SH, the agreement between the two is obviously much, much closer than that from model A (see Fig. 2(a)). We tentatively conclude that, for this two-dimensional problem, similar to what was found in ref. 42 for a one-dimensional problem, EF-LD agrees with SH dynamics when the problem is effectively one dimensional and the trajectories proceed through an area where the velocities are thermally equilibrated.

C. Model C

Our final example investigates the case where multiple reaction channels exist and the coupling and reaction coordinate are mixed. Fig. 4(b) shows the PMF for model C, while Fig. 4(c) shows the "effective" force on a particle in the positive y-direction, assuming a positive x velocity and negative y velocity with magnitude equal to the root-mean square velocity. One expects that the minima centered near $+y_A$ will be favored when $\Delta G^\circ_R = \Delta G^\circ_L$, since the coupling $\Gamma(y)$ is higher for $y > 0$. However, as the energy difference is increased by lowering ΔG°_L, we expect to see more trajectories equilibrate in the minima centered at $-y_A$. To test this, we change the value of ΔG°_L and monitor what fraction of trajectories finish in each minima for both SH and EF-LD.

Fig. 5(a) shows the ratio of trajectories in each of the two product wells at long times as a function of ΔG°_L. We find that, as the energy bias grows, EF-LD does not recover the correct statistics at long times. Presumably, this failure of EF-LD is caused by the kinetic barrier introduced by the low coupling/high friction separating the two minima (see Fig. 4(c)). This barrier will result in EF-LD subsequently underestimating the correct ET rate, as shown in Fig. 5(b).

In Fig. 5(c) and (d) we address the question of non-Condon effects and study the equilibrium population and trajectory data when Γ is kept constant, equal to Γ_1. In this case, EF-LD yields much more similar rates and equilibrium populations compared to SH: thus, the existence of non-Condon effects strongly strains the ability of EF-LD dynamics to recover the

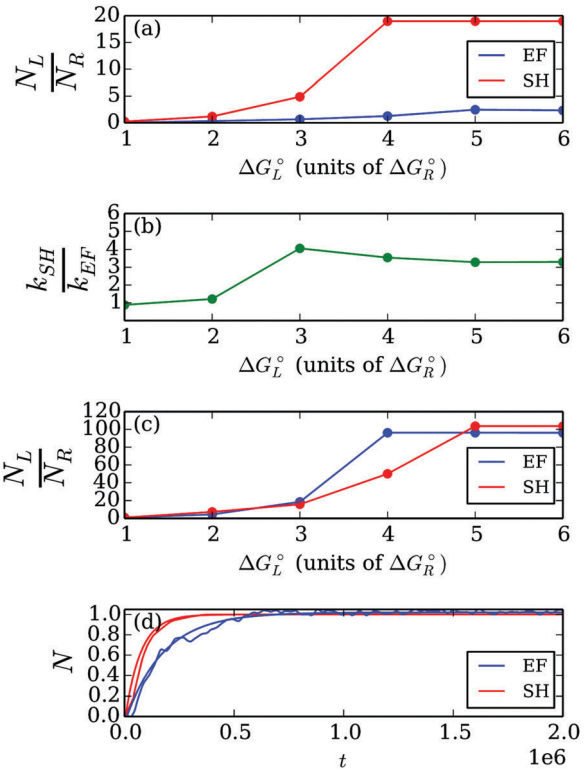

Fig. 5 Results for model C. (a) Ratio of number of trajectories in left minima *versus* right minima for SH and EF-LD (ω_y = 5ω = 0.001, $\Delta G_R^\circ = -0.0038$, y_A = 5, Γ_0 = 2e − 5, κ = 5) with ΔG_L° varying (ΔG_L° in units of ΔG_R°). Note that EF-LD fails for large ΔG_L°. (b) Ratio of overall rates for reactant going to product (either product basin) for SH and EF-LD for the model in (a), with ΔG_L° varying (ΔG_R° in units of ΔG_R°). (c) Ratio of number of trajectories in left minima *versus* right minima for SH and EF-LD with parameters from (a), except with constant $\Gamma(y) = \Gamma_1$. Note that EF-LD performs quite well for cases when the Condon approximation is not violated. (d) Time data for determining and fitting the overall rate for SH and EF-LD for $\Delta G_L^\circ = 6\Delta G_R^\circ$ for the model in (a), except with constant $\Gamma(y) = \Gamma_1$. Again, EF-LD performs well.

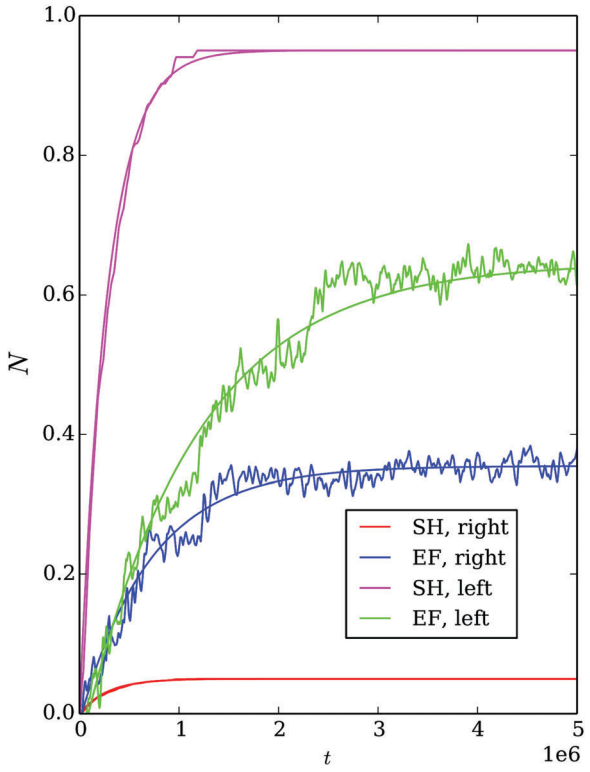

Fig. 6 The fraction of trajectories in each product basin as a function of time and fits according to SH and EF-LD for $\Delta G_L^\circ = 6\Delta G_R^\circ$ for model C. All other parameters are the same as in Fig. 5. Note that both the rate and the equilibrium population in each minima are vastly different, demonstrating that EF-LD fails in this case.

correct relative rates of transfer. After all, when the metal–molecule coupling changes significantly, the electronic friction can change dramatically as well. However, within the Condon approximation, EF-LD can treat the competition between two pathways far better apparently.

Finally, Fig. 6 plots the population in the product basins as a function of time for $\Delta G_L^\circ = 6\Delta G_R^\circ$ for the parameters in Fig. 5(a and b) (*i.e.* with Γ depending on y). Both the rates and final populations in each minima differ greatly between the two methods, suggesting that EF-LD is not suitable for these dynamics.

IV. Discussion

In this paper we have worked in the limit of weak molecule–metal and we have used three different models to assess when EF-LD is a valid description of dynamics. We have found that the validity of EF-LD seems directly tied to the separability of the reaction coordinate and the nuclear direction that breaks the Condon approximation. If the reaction pathway and coupling coordinate are identical, as in model A, then EF-LD will not recover the correct dynamics, as evinced by the large disagreement in rates between SH and EF-LD for a wide set of model parameterizations (see Fig. 2(a)). This disagreement is empirically tied to the presence of a bimodal hopping distribution. For model B, however, where the coupling and reaction coordinates are not entangled, Fig. 3(a) shows good agreement between rates of ET for SH and EF-LD, revealing that EF-LD can succeed as long as equilibration is fast with respect to the reaction coordinate. Finally, if we mix the reaction and coupling coordinates, as illustrated by model C, Fig. 5 and 6 show that EF-LD again fails to recover the correct rate and populations. In this case, again, there are two reactive pathways that compete for trajectories, and EF-LD clearly fails if one cannot rely on the Condon approximation.

Now, let us reconsider the theoretical argument in ref. 42. In that paper, using transition state theory, the authors showed that an adiabatic EF-LD reaction rate was consistent with Marcus's nonadiabatic rate theory if we assumed a single reactive coordinate, equilibrated velocities, and constant Γ. This equivalence was shown using Kramer's theory for an adiabatic EF-LD reaction rate in the limit of large friction. With this fact in mind, we would like to revisit the original proof in ref. 42 in the context of a multidimensional Hamiltonian. As in ref. 42 we work exclusively in the high friction (overdamped) limit, and in

order to make a simple analytical argument, we will also work in the limit of near separability between reaction and bath coordinates.

With these assumptions in mind, we begin with the multidimensional Smoluchowski equation,

$$\frac{\partial P(\mathbf{x},t)}{\partial t} = \nabla \cdot \mathbf{D}(\mathbf{x}) \cdot [\nabla + \beta \nabla U(\mathbf{x})] P(\mathbf{x},t) \tag{17}$$

where $P(\mathbf{x},t)$ is the probability density, $\mathbf{D}(\mathbf{x})$ is the multidimensional diffusion tensor, and $U(\mathbf{x})$ is the potential, which corresponds to a reactive flux

$$\mathbf{J}(\mathbf{x},t) = -\mathbf{D}(\mathbf{x}) \cdot [\nabla + \beta \nabla U(\mathbf{x})] P(\mathbf{x},t). \tag{18}$$

Since we desire a steady-state solution for $P(\mathbf{x},t) = P_{ss}(\mathbf{x})$, with vanishing probability as $|\mathbf{x}| \rightarrow \infty$, we assume the following functional form for the steady-state probability:

$$P_{ss}(\mathbf{x}) = f(\mathbf{x}) e^{-\beta U(\mathbf{x})}. \tag{19}$$

Taking the gradient of both sides and substituting $\nabla P_{ss}(\mathbf{x})$ into eqn (18) yields

$$\mathbf{J}(\mathbf{x}) = -\mathbf{D}(\mathbf{x}) \cdot [\nabla f e^{-\beta U(\mathbf{x})}]. \tag{20}$$

At this point, we assume that the diffusion tensor is invertible, such that

$$\nabla f = -\mathbf{D}(\mathbf{x})^{-1} \cdot \mathbf{J}(\mathbf{x}) e^{\beta U(\mathbf{x})}. \tag{21}$$

We now further assume that $\{\mathbf{x}\} = \{\mathbf{Q}\} + \{\mathbf{s}\}$, where $\{\mathbf{s}\}$ is the reaction coordinate and $\{\mathbf{Q}\}$ are the remaining bath coordinates. Because the reaction rate is determined by motion along s, which may depend on Q (though only weakly in the limit of near separability), we integrate both sides over a path s' (which may depend on Q),

$$f(\mathbf{s},\mathbf{Q}) = -\int_{\infty}^{s} d\mathbf{s}' \cdot \mathbf{D}(\mathbf{s}',\mathbf{Q})^{-1} \cdot \mathbf{J}(\mathbf{s}',\mathbf{Q}) e^{\beta U(\mathbf{s}',\mathbf{Q})}. \tag{22}$$

Finally, at steady state where $\mathbf{J}$ is a constant, given our assumption of near separability between reaction and bath coordinates, we expect $\mathbf{J}(\mathbf{s},\mathbf{Q}) = \mathbf{J}(\mathbf{Q}) = |J(\mathbf{Q})|\hat{s}$ and thus:

$$f(\mathbf{s},\mathbf{Q}) = |J(\mathbf{Q})| \int_{s}^{\infty} ds' (\hat{s}' \cdot \mathbf{D}(\mathbf{s}',\mathbf{Q})^{-1} \cdot \hat{s}') e^{\beta U(\mathbf{s}',\mathbf{Q})}. \tag{23}$$

Now, to find the rate, we evaluate the flux divided by the population for every bath coordinate,

$$\begin{aligned} k(\mathbf{Q}) &= \frac{|J(\mathbf{Q})|}{\int_{-\infty}^{s_B} ds P_{ss}(\mathbf{s},\mathbf{Q})} \\ k(\mathbf{Q}) &= \left[\int_{-\infty}^{s_B} ds e^{-\beta U(\mathbf{s},\mathbf{Q})} \int_{s}^{\infty} ds' \beta \gamma_e^{s's'} e^{\beta U(\mathbf{s}',\mathbf{Q})} \right]^{-1} \end{aligned} \tag{24}$$

where we have used the relationship $\gamma_e \cdot \mathbf{D} = \mathbf{D} \cdot \gamma_e = \beta^{-1}\hat{1}$ to replace the element of the diffusion tensor with the corresponding element of the friction tensor. Obviously, $k(\mathbf{Q})$ is a simple 1D rate constant analagous to the rate in ref. 42:

$$k^{1D} = \left[\int_{-\infty}^{s_B} ds e^{-\beta U(s)} \int_{s}^{\infty} ds' \beta \gamma_e e^{\beta U(s')} \right]^{-1}. \tag{25}$$

And, as shown in ref. 42, this expression is equivalent to the following expression in the limit of small Γ (where γ_e is effectively a delta function), which is also equivalent to Marcus theory:

$$k^{1D} \approx \frac{1}{Z_0} \frac{\Gamma}{\beta\hbar} \left| \frac{dE(s)}{ds}|_{s=s_B} \right| e^{-\beta U(s_B)}. \tag{26}$$

Thus, in the end we have shown that a multidimensional problem with electronic friction can still be reduced to Marcus theory. However, a few conditions must be met. First, the potential $U(\mathbf{s},\mathbf{Q})$ must be separable in the reaction and bath coordinates, $U(\mathbf{s},\mathbf{Q}) = U(\mathbf{s}) + U(\mathbf{Q})$, and the difference in energy $E = U_1 - U_0$ must be independent of Q. Second, $\gamma_e^{s's'}$ must equal $\frac{\beta\hbar}{\Gamma} f(E(\mathbf{s},\mathbf{Q}))(1 - f(E(\mathbf{s},\mathbf{Q})))\left(\frac{dE}{ds}\right)^2$, which only occurs when Γ is constant with respect to the reaction coordinate s. In other words, given our assumption of near separability, one can break the Condon approximation, but only in the Q-direction, not the s-direction, (*i.e.* $\frac{\partial \Gamma}{\partial s}$ must be zero, but $\frac{\partial \Gamma}{\partial Q}$ can be nonzero). Overall, this heuristic argument provides a mathematical justification for the results we have found above for models A, B, and C. For model B, where the conditions above hold, we find that EF-LD recovers SH results. This equivalence does not hold for model A or model C, where the reaction coordinate and the coordinate over which Γ varies are either identical or mixed, respectively.

V. Conclusions

In the end, whereas ref. 42 demonstrated analytically that EF-LD will fail if there are excited state dynamics, the present results suggest something more general: EF-LD may fail if there are two different, non-equivalent pathways—along the ground or excited states—consistent with different hopping locations in phase space and different metal–molecule couplings. In other words, we have found that (i) separability of the reaction and bath coordinates and (ii) the validity of the Condon approximation in the reaction coordinate are not only sufficient but also necessary if one wishes to safely invoke EF-LD trajectories. Furthermore, we remind the reader that transition state theory does not have any validity without external friction and equilibrated velocities, and thus EF-LD cannot agree with SH without any external friction for weak molecule–metal coupling.[12,42] Thus, in the end, the promising analytic transition state theory result in ref. 42 that allowed Kramer's theory to recover the Marcus theory result in the nonadiabatic limit would appear to be a very limited success story.

Looking forward, the most natural next step is to begin investigating both *ab initio* and model problems with increasing numbers of nuclear coordinates, where we may test the electronic friction approach in a truly condensed phase environment. In particular, we would like to apply EF-LD trajectories to the case of electron transfer at metal surfaces but, as a practical matter, we must first ascertain how the metal–molecule coupling

changes for realistic problems and learn when multiple pathways are possible (which is likely the case for radical chemistry). Many exciting questions remain regarding the intersection of electronic structure theory and nonadiabatic dynamics at metal surfaces.

Conflicts of interest

There are no conflicts to declare.

References

1 M. Silva, R. Jongma, R. W. Field and A. M. Wodtke, *Annu. Rev. Phys. Chem.*, 2001, **52**, 811.
2 A. M. Wodtke, J. C. Tully and D. J. Auerbach, *Int. Rev. Phys. Chem.*, 2004, **23**, 513.
3 O. Bunermann, H. Jiang, Y. Dorenkamp, A. Kandratsenka, S. M. Janke, D. J. Auerbach and A. M. Wodtke, *Science*, 2015, **350**, 1346.
4 B. C. Krüger, S. Meyer, A. Kandratsenka, A. M. Wodtke and T. Schäfer, *J. Phys. Chem. Lett.*, 2016, **7**, 441.
5 A. M. Wodtke, *Chem. Soc. Rev.*, 2016, **45**, 3641.
6 S. Gosavi and R. Marcus, *J. Phys. Chem. B*, 2000, **104**, 2067.
7 J. H. Mohr and W. Schmickler, *Phys. Rev. Lett.*, 2000, **84**, 1051.
8 S. Hammes-Schiffer and A. V. Soudackov, *J. Phys. Chem. B*, 2008, **112**, 14108.
9 W. Ouyang, J. G. Saven and J. E. Subotnik, *J. Phys. Chem. C*, 2015, **119**, 20833.
10 Y. Huang, C. T. Rettner, D. J. Auerbach and A. M. Wodtke, *Science*, 2000, **290**, 111.
11 C. Bartels, R. Cooper, D. J. Auerbach and A. M. Wodtke, *Chem. Sci.*, 2011, **2**, 1647.
12 W. Dou, A. Nitzan and J. E. Subotnik, *J. Chem. Phys.*, 2015, **142**, 084110.
13 W. Dou, A. Nitzan and J. E. Subotnik, *J. Chem. Phys.*, 2015, **143**, 054103.
14 E. G. D'Agliano, P. Kumar, W. Schaich and H. Suhl, *Phys. Rev. B: Solid State*, 1975, **11**, 2122.
15 M. Head-Gordon and J. C. Tully, *J. Chem. Phys.*, 1992, **96**, 3939.
16 M. Head-Gordon and J. C. Tully, *J. Chem. Phys.*, 1995, **103**, 10137.
17 M. S. Mizielinski, D. M. Bird, M. Persson and S. Holloway, *J. Chem. Phys.*, 2005, **122**, 084710.
18 M. S. Mizielinski, D. M. Bird, M. Persson and S. Holloway, *J. Chem. Phys.*, 2007, **126**, 034705.
19 B. B. Smith and J. T. Hynes, *J. Chem. Phys.*, 1993, **99**, 6517.
20 V. Krishna, *J. Chem. Phys.*, 2006, **125**, 034711.
21 M. Plihal and D. Langreth, *Phys. Rev. B: Condens. Matter Mater. Phys.*, 1998, **58**, 2191.
22 M. Plihal and D. Langreth, *Phys. Rev. B: Condens. Matter Mater. Phys.*, 1999, **60**, 5969.
23 N. Bode, S. V. Kusminskiy, R. Egger and F. von Oppen, *Beilstein J. Nanotechnol.*, 2012, **3**, 144.
24 M. Thomas, T. Karzig, S. V. Kusminskiy, G. Zaránd and F. Von Oppen, *Phys. Rev. B: Condens. Matter Mater. Phys.*, 2012, **86**, 195419.
25 M. Galperin and A. Nitzan, *J. Phys. Chem. Lett.*, 2015, **6**, 4898.
26 M. Brandbyge, P. Hedegård, T. F. Heinz, J. A. Misewich and D. M. Newns, *Phys. Rev. B: Condens. Matter Mater. Phys.*, 1995, **52**, 6042.
27 J. Daligault and D. Mozyrsky, *Phys. Rev. E: Stat., Nonlinear, Soft Matter Phys.*, 2007, **75**, 026402.
28 D. Mozyrsky, M. B. Hastings and I. Martin, *Phys. Rev. B: Condens. Matter Mater. Phys.*, 2006, **73**, 035104.
29 W. Dou and J. E. Subotnik, *J. Chem. Phys.*, 2017, **146**, 092304.
30 W. Dou, G. Miao and J. E. Subotnik, *Phys. Rev. Lett.*, 2017, **119**, 046001.
31 W. Dou and J. E. Subotnik, *Phys. Rev. B*, 2017, **96**, 104305.
32 C. Martens and J.-Y. Fang, *J. Chem. Phys.*, 1997, **106**, 4918.
33 R. Kapral and G. Ciccotti, *J. Chem. Phys.*, 1999, **110**, 8919.
34 V. Romero-Rochin, A. Orsky and I. Oppenheim, *Phys. A*, 1989, **156**, 244.
35 V. Romero-Rochin and I. Oppenheim, *Phys. A*, 1989, **155**, 52.
36 W. Dou and J. E. Subotnik, *J. Chem. Phys.*, 2016, **144**, 024116.
37 N. Shenvi, S. Roy and J. C. Tully, *J. Chem. Phys.*, 2009, **130**, 174107.
38 N. Shenvi, S. Roy and J. C. Tully, *Science*, 2009, **326**, 829.
39 S. Li and H. Guo, *J. Chem. Phys.*, 2002, **117**, 4499.
40 S. Monturet and P. Saalfrank, *Phys. Rev. B: Condens. Matter Mater. Phys.*, 2010, **82**, 075404.
41 S. P. Rittmeyer, J. Meyer, J. I. Juaristi and K. Reuter, *Phys. Rev. Lett.*, 2015, **115**, 046102.
42 W. Ouyang, W. Dou, A. Jain and J. E. Subotnik, *J. Chem. Theory Comput.*, 2016, **12**, 4178.
43 G. Miao, W. Dou and J. E. Subotnik, *J. Chem. Phys.*, 2017, **147**, 224105.
44 T. Holstein, *Ann. Phys.*, 1959, **8**, 343.
45 P. W. Anderson, *Phys. Rev.*, 1961, **124**, 41.
46 R. Zwanzig, *Nonequilibrium statistical mechanics*, Oxford University Press, 2001.
47 There is a curious result in Fig. 2(a) in the case of $K = 0.001$. Here, we see that the ratio of the SH rate over the EF-LD rate is maximized when $\Gamma_0 = 0.1$ and then decreases again as Γ_0 decreases further. This state of affairs is actually consistent with the other data provided in the body of this paper. A detailed analysis shows that, for $K = 0.001$, the surface hopping distribution is more bimodal at $\Gamma_0 = 0.1$ and less bimodal at $\Gamma_0 = 0.01$.

